Supporting Information

Boosting Solar Hydrogen Production with Polarized MOF-Derived Ferroelectric In_2Se_3/In_2O_3 Nanohybrids

Li Shi[a,b], Daniele Benetti[a,c]*, Faying Li[a,b], Catalin Harnagea[a], Qin Wei[b,d]*, and Federico Rosei[a,e]*

[a] *Centre for Energy, Materials and Telecommunications, Institut National de la Recherche Scientifique, 1650 Boul. Lionel-Boulet, Varennes, QC J3X1S2, Canada*

[b] *Key Laboratory of Interfacial Reaction & Sensing Analysis in Universities of Shandong, School of Chemistry and Chemical Engineering, University of Jinan, Jinan 250022, PR China*

[c] *Department of Chemistry, McGill University, 801 Sherbrooke Street West, Montreal, Quebec, H3A 0B8 Canada*

[d] *Department of Chemistry, Sungkyunkwan University, Suwon, 16419, Republic of Korea*

[e] *Department of Chemical and Pharmaceutical Sciences, University of Trieste, Via Giorgeri 1, 34127 Trieste (Italy)*

* Corresponding author: daniele.benetti@inrs.ca (D.B.) Present Address: Department of Chemistry, Imperial College London, W12 0BZ, London, United Kingdom; chm_weiq@ujn.edu.cn (Q.W.); federico.rosei@units.it (F.R.)

Table of Contents

EXPERIMENTAL DETAILS

Synthesis of MIL-68(In)-MOFs nanorod precursor: A modified version of MIL-68(In) was prepared according to previous literature[1]. Typically, a mixture milky solution was prepared by mixing 1,4-benzenedicarboxylic acid (H_2BDC, 0.8 mol, 32 mg) and $In(NO_3)_3$ xH_2O (0.8 mol, 256 mg) in 30 mL of DMF. Afterwards, the mixture was heated in an oil bath (120 °C) for 30 mins. Upon cooling down, the final white products were centrifuged and washed with DMF and methanol three times, respectively. The collected materials were then dried in an oven overnight at 80 °C.

***Synthesis of pure In_2O_3 and ferroelectric x%-In_2Se_3/In_2O_3*:** 0.5 g of the MIL-68(In) powder was annealed in a tube furnace in N_2 atmosphere to 500 °C with a ramp-rate of 2 °C/min and held for 120 min. After naturally cooling, black powders of pure In_2O_3 were obtained. MIL-68(In) nanorod and Se powder with different mass ratios (0%, 20%, and 40%) were uniformly mixed by grinding with a mortar and pestle. Then, the mixture was transferred to a porcelain boat and heated at 500 °C for 2 h with a ramping rate of 2 °C/min in nitrogen atmosphere. After naturally cooling, brown powders of pure In_2Se_3/In_2O_3 were obtained. When the mass ratio of Se to MIL-68(In) is 40%, which is marked 40%-In_2Se_3/In_2O_3, there will be only In_2Se_3 exist (dark red) (see details in Figure. S1).

***Online gas chromatography to measure the H_2 evolution**:* A gas-tight cell (total volume: 50 mL) was used for online gas chromatography (GC) and it was filled with 20 mL electrolyte in a three-electrode cell configuration, using a M-TiO_2/CdSe@CdS photoanode as working electrode, an Ag/AgCl saturated reference electrode and a Pt plate as working electrode. Ar was used as carrier gas at a flow rate of 20 sccm and the electrolyte was continuously stirred. Before the measurements, the electrolyte was saturated with Ar gas for at least 30 minutes. A gas outlet was connected to a gas chromatograph (Perkin Elmer Clarus 580 GC) for periodical sampling. A thermal conductivity detector (TCD) was used for detecting H_2. A gas aliquot was automatically injected into the GC every 180 s. During the online GC, a chronoamperometric measurement was performed by applying a 1.4 V vs RHE potential for 1.5 h.

The theoretical number of moles of hydrogen evolved can be calculated from Faraday's 2nd law of electrolysis according to the following equation:

$$n_{H_2}(\text{theoretical}) = \frac{Q}{zF} = \frac{I \times t}{zF}$$

Where n_{H_2} is the number of moles of hydrogen produced, Q is the total charge passed during electrolysis, z is the number of electrons transferred during HER (i.e. $z = 2$), I is the applied current, t is the electrolysis time in seconds, and F is the Faraday constant 96 485.33 C mol^{-1}.

The Faradaic efficiency was calculated as follows:

$$\eta_{Faradaic} = \frac{n_{H_2}(\text{experimental})}{n_{H_2}(\text{theoretical})} \times 100\%$$

For example, according to gas chromatography after 5400s, the H_2 gas evolved was 5.847×10^{-6} mol, whereas the current obtained by chronoamperometry is 0.26 mA.

$$n_{H_2}(\text{theoretical}) = \frac{0.00026\ (A) \times 5400\ (s)}{2 \times 96485.33\ C \cdot mol^{-1}} = 7.27 \times 10^{-6}\ mol$$

Consequently,

$$\eta_{Faradaic} = \frac{5.85 \times 10^{-6}\, mol}{7.27 \times 10^{-6}\, mol} = 80.47\%$$

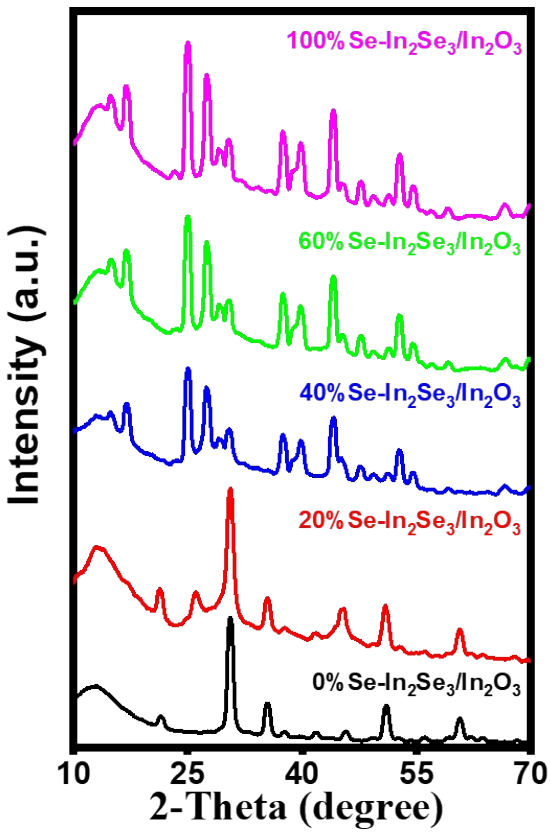

Figure S1. Comparative XRD patterns of In_2O_3 (0%-In_2Se_3/In_2O_3), 20%-In_2Se_3/In_2O_3, 40%-In_2Se_3/In_2O_3, 60%-In_2Se_3/In_2O_3, 80%-In_2Se_3/In_2O_3, In_2Se_3 (100%-In_2Se_3/In_2O_3).

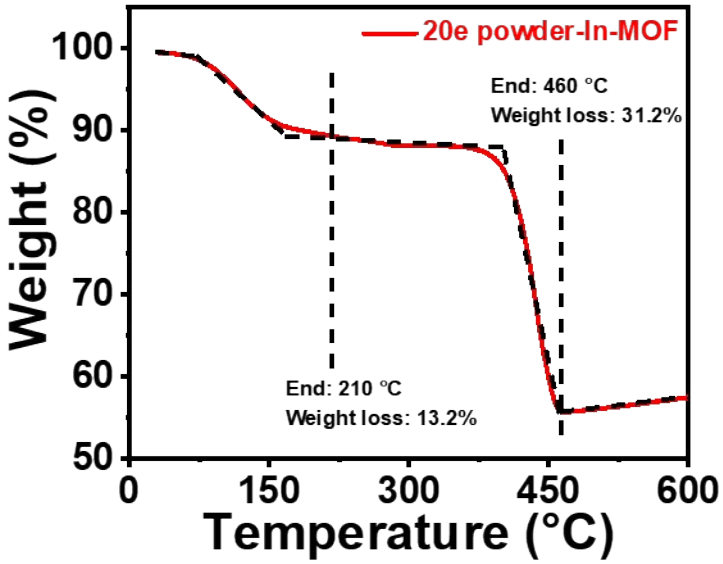

Figure S2. TGA curves of the as-obtained 20% Se powder-MIL-68(In).

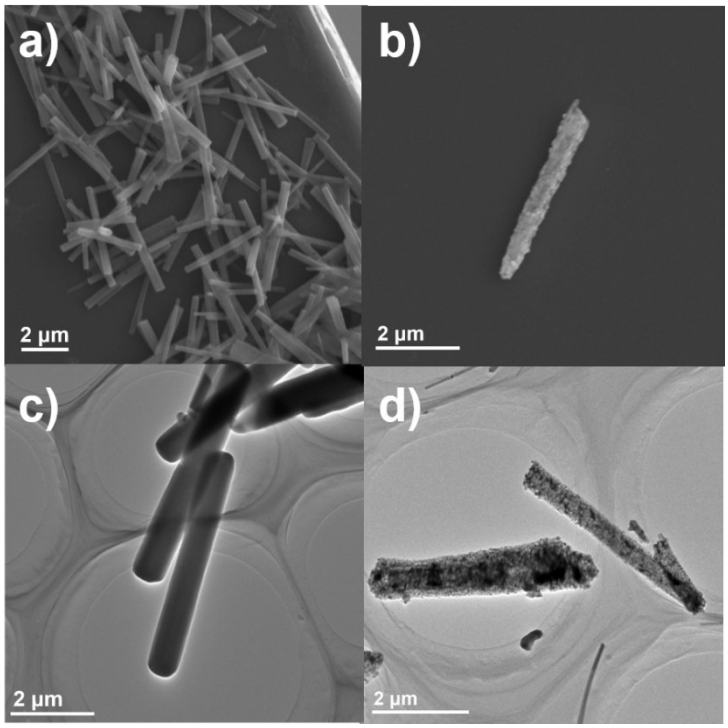

Figure S3. SEM and TEM images of In-MIL-68 (a and c) and 20%-In_2Se_3/In_2O_3 composite (b and d).

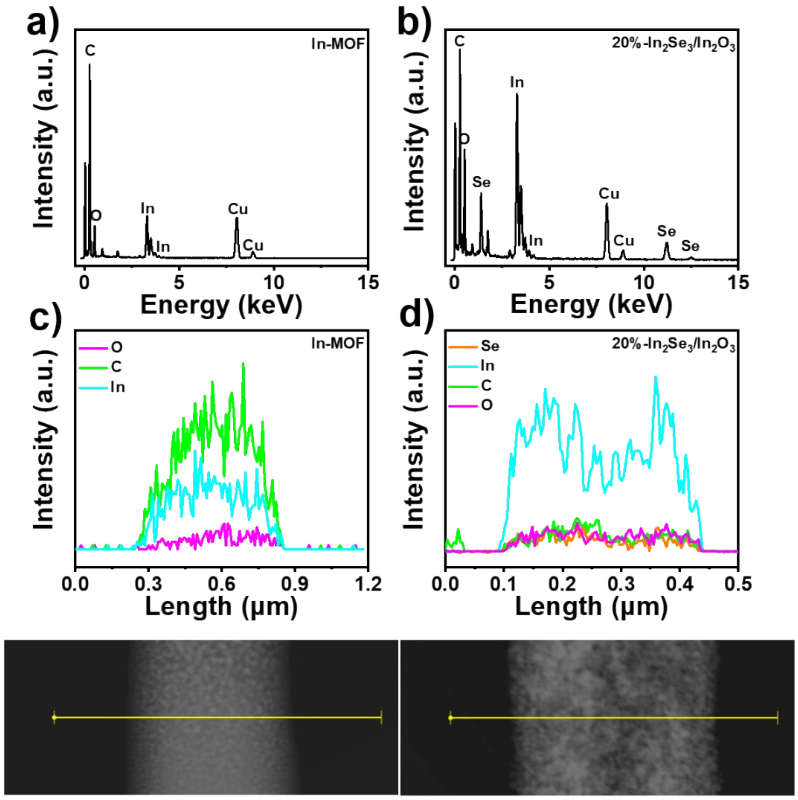

Figure S4. EDX spectrum of In-MIL-68 (a) and 20%-In_2Se_3/In_2O_3 composite (b) (Cu substrate). EDX line scan of In-MIL-68 (c) and 20%-In_2Se_3/In_2O_3 composite (d).

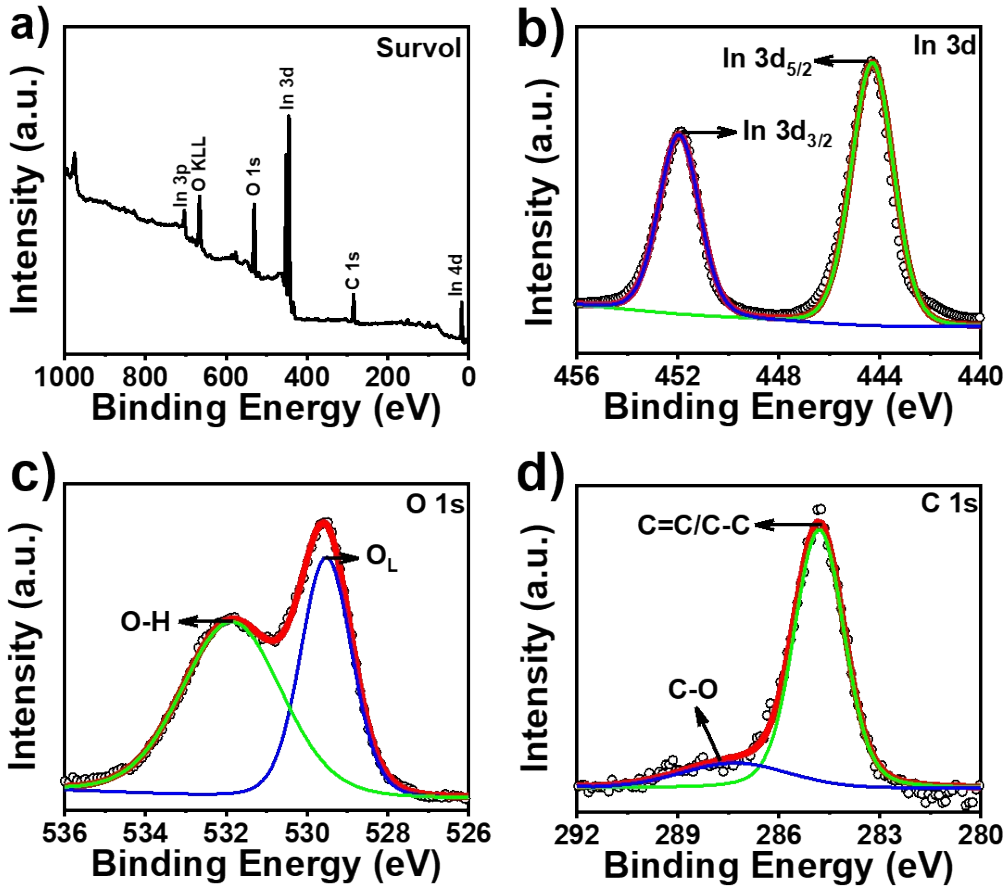

Figure S5. XPS survey spectra of (a) In_2O_3. High resolution In 3d spectra (b). High resolution O 1s spectra (c) and (d) High resolution C 1s spectra.

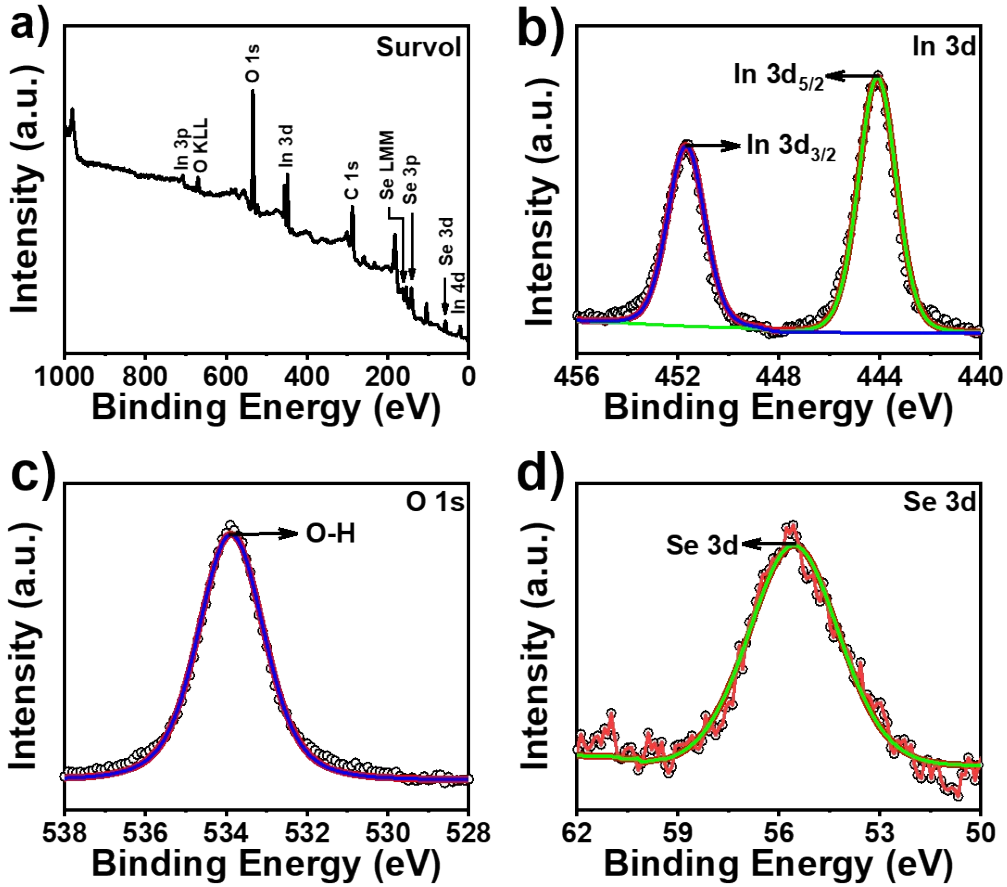

Figure S6. XPS survey spectra of (a) In_2Se_3. High resolution In 3d spectra (b). High resolution O 1s spectra (c) and (d) High resolution C 1s spectra.

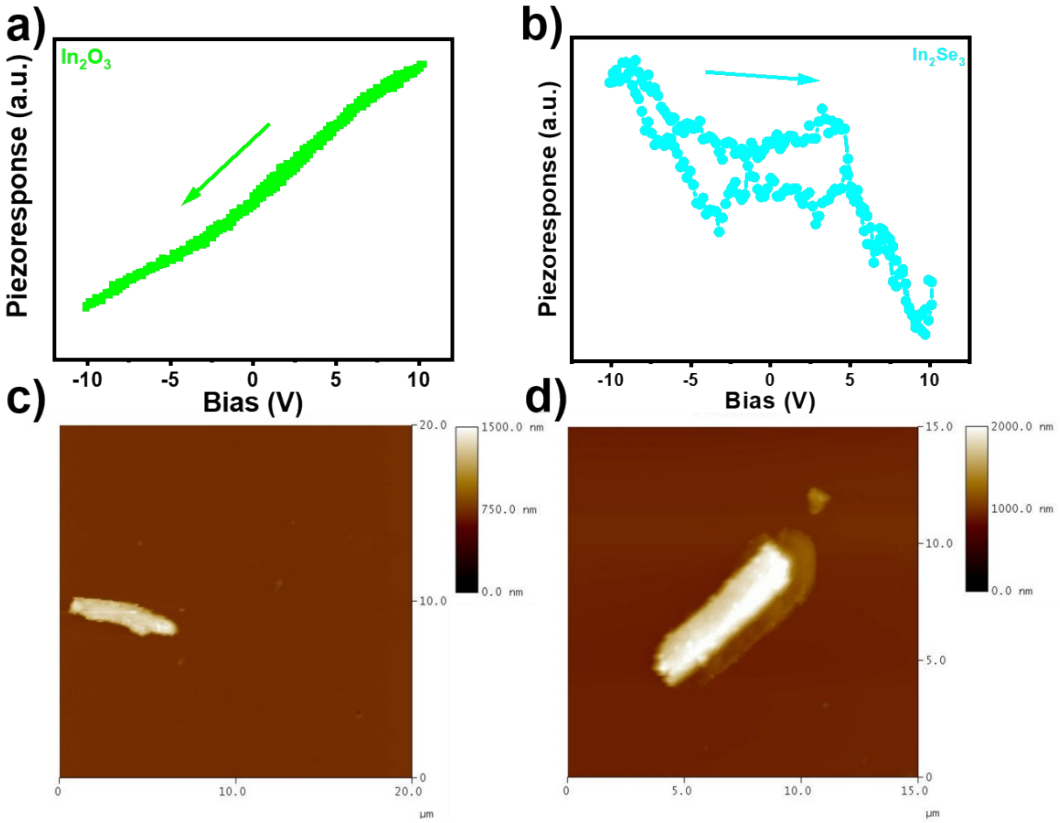

Figure S7. (a and b) Local ferroelectric hysteresis loops for In_2O_3 and In_2Se_3 nanorods; (c and d) AFM topographic image representation of an individual In_2O_3 and In_2Se_3 nanorods lying on Pt coated silicon substrate surface.

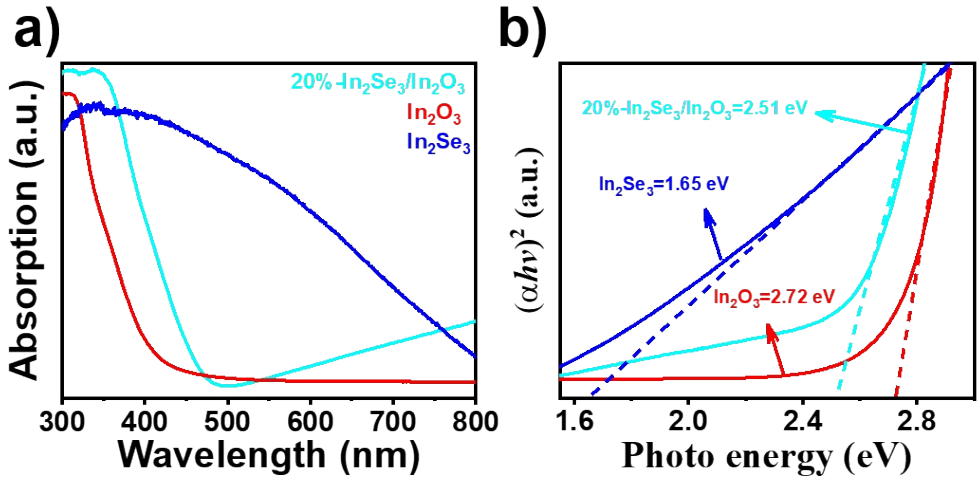

Figure S8. (a) UV-DRS spectra of In_2O_3, 20%-In_2Se_3/In_2O_3, and In_2Se_3 (b) The extrapolation of Tauc plots ($(\alpha hv)^2$ versus photon energy (hv)) for In_2O_3, 20%-In_2Se_3/In_2O_3, and In_2Se_3.

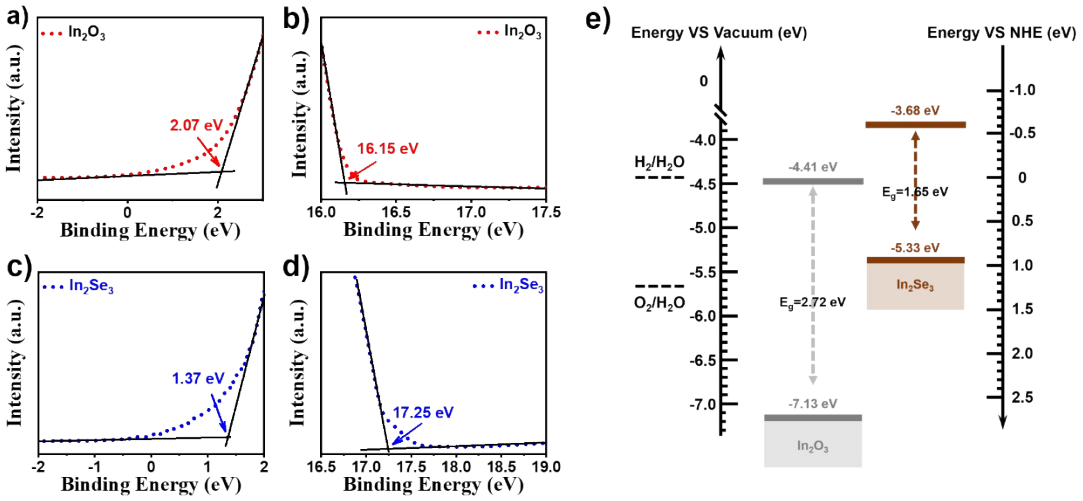

Figure S9. High binding energy cut-off (a and c) and low binding energy cut-off (b and d) of UPS spectra of In_2O_3 and In_2Se_3. (e) Summary of the energy levels obtained from UPS measurements.

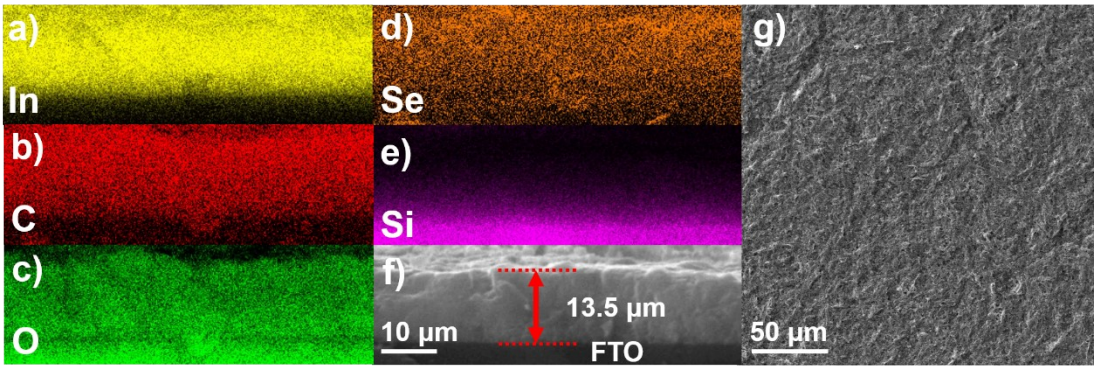

Figure S10. plain-view and cross-sectional SEM image of 20%-In_2Se_3/In_2O_3 composite (f and g); EDS mapping analysis of all the elements in relevant 20%-In_2Se_3/In_2O_3 electrode including (a) In, (b) C, (c) O, (d) Se, (e) Si.

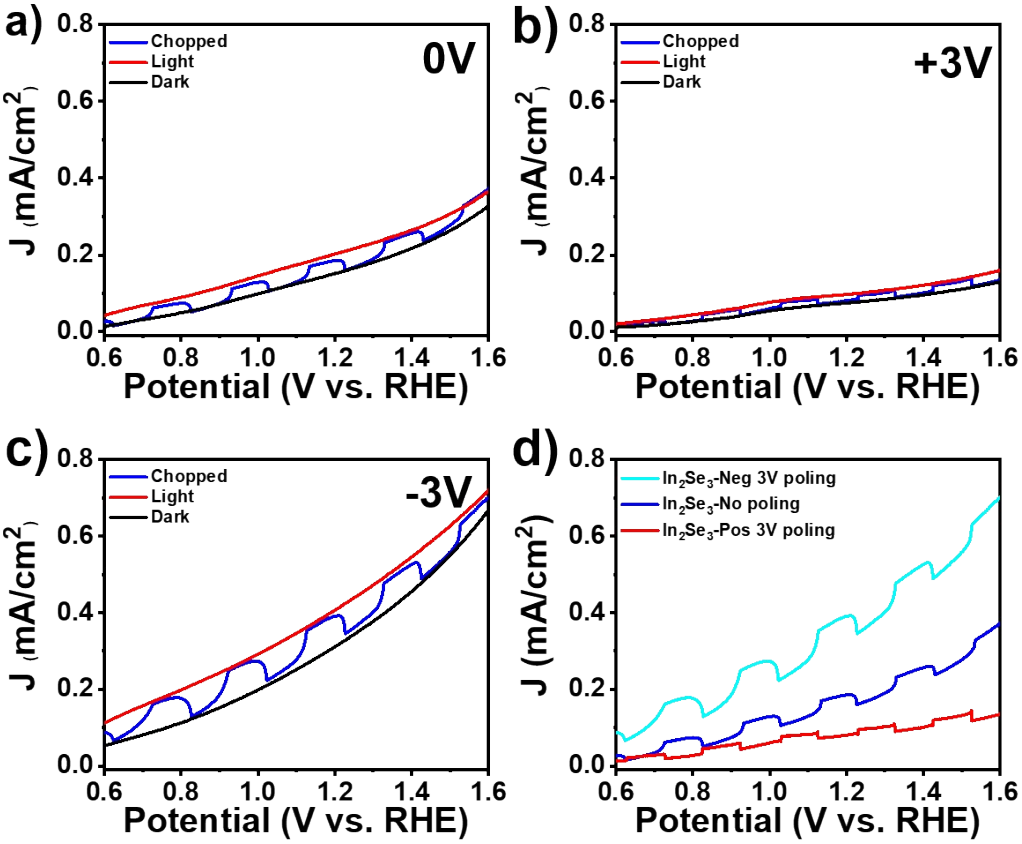

Figure S11. Photocurrent density of (a) In_2Se_3 with no poling; (b) In_2Se_3 with +3 V poling; (c) In_2Se_3 with -3 V poling under dark, continuous and chopped illumination (AM 1.5 G, 100 mW cm^{-2}); (d) Summary of chopped illumination of In_2Se_3 with no poling, +3 V poling, and -3 V poling.

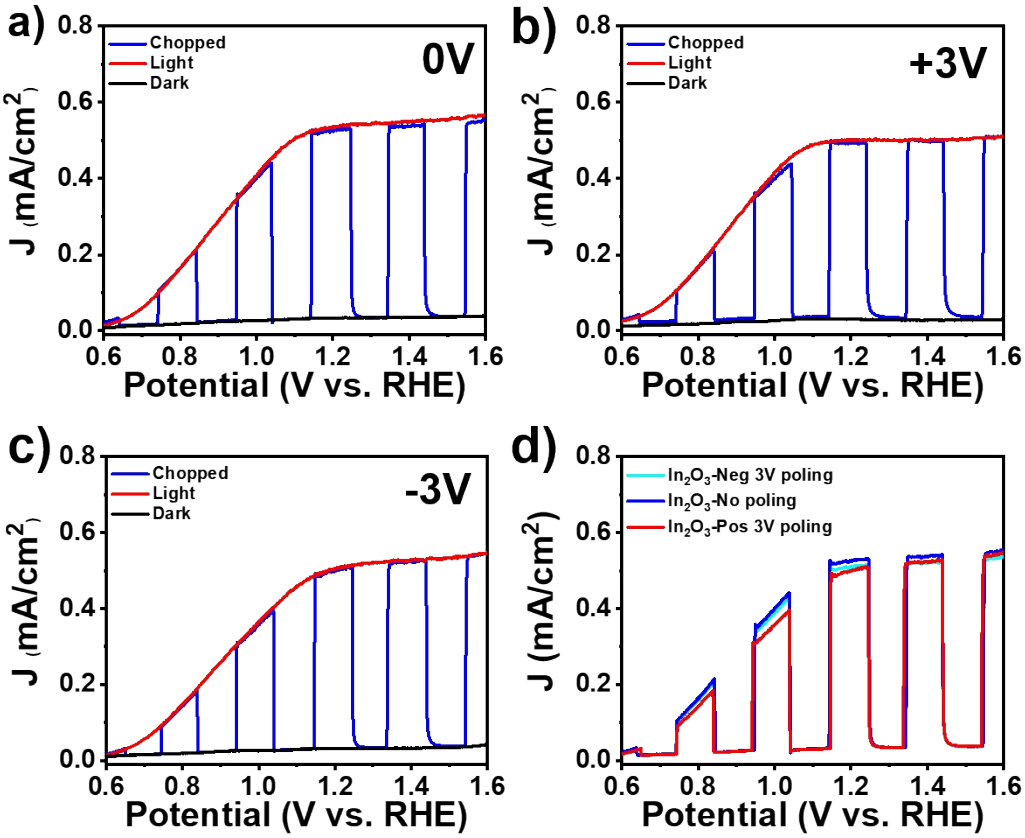

Figure S12. Photocurrent density of (a) In_2O_3 with no poling; (b) In_2O_3 with +3 V poling; (c) In_2O_3 with -3 V poling under dark, continuous and chopped illumination (AM 1.5 G, 100 mW cm^{-2}); (d) Summary of chopped illumination of In_2O_3 with no poling, +3 V poling, and -3 V poling.

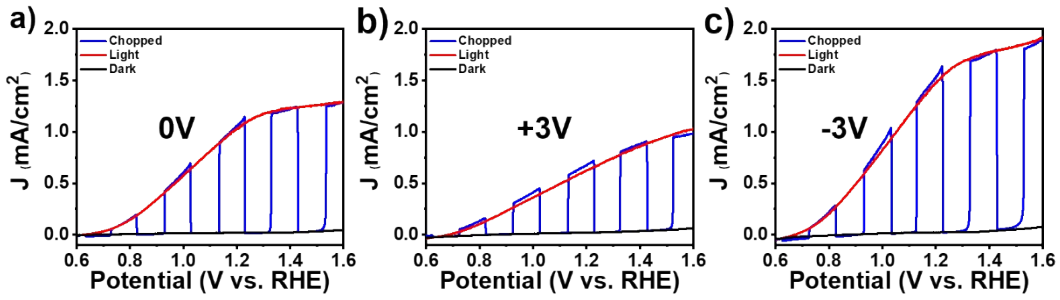

Figure S13. Photocurrent density of (a) 20%-In_2Se_3/In_2O_3 with no poling; (b) 20%-In_2Se_3/In_2O_3 with +3 V poling; (c) 20%-In_2Se_3/In_2O_3 with -3 V poling under dark, continuous and chopped illumination (AM 1.5 G, 100 mW cm^{-2});

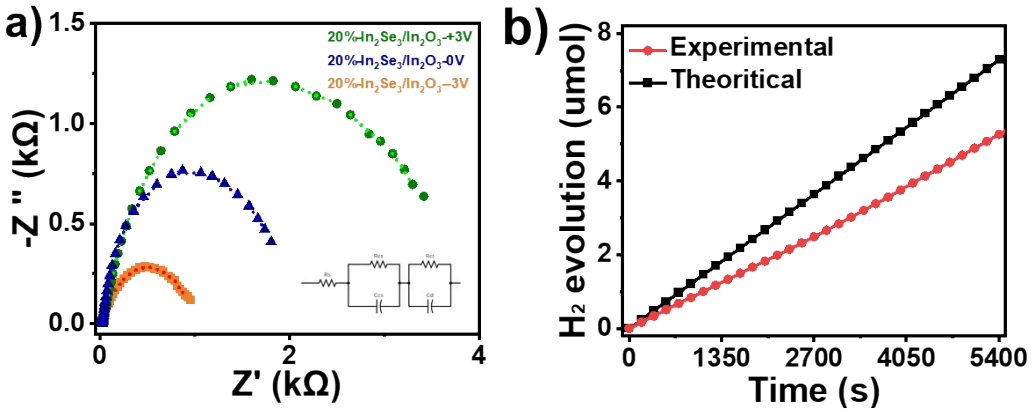

Figure S14. (a) Nyquist plots of 20%-In_2Se_3/In_2O_3 with 0 V poling, -3 V poling, and +3 V poling (the inset is equivalent circuit). (b) H_2 evolution of 20%-In_2Se_3/In_2O_3 composite as a function of time at 1.4 V vs RHE under 100 mW/cm^2 illumination with AM 1.5 G filter. The evolution of H_2 exhibits a nearly linear increase over time (solid red curve, approximately 3.72 μmol/h). H_2 evolution is also calculated from the measured current (solid black curve).

Table S1 the values of the R_{CT}

Sample	R_{ct} (kΩ)
20%-In_2Se_3/In_2O_3 + 3 V	38.46
20%-In_2Se_3/In_2O_3 0 V	24.73
20%-In_2Se_3/In_2O_3 - 3 V	17.71

Table S2 Comparison of the PEC performance of some representative In_2O_3 photocatalysts with literature

Photocathode	Electrolyte	Light Source	Photocurrent density (mA cm^{-2})	Ref.
In_2O_3	**1 M NaOH**	**1 Sun**	**0.36 (1.6 V vs RHE)**	**Present work**
In_2Se_3	**1 M NaOH**	**1 Sun**	**0.7 (1.6 V vs RHE)**	**Present work**
20% In_2Se_3/In_2O_3 (+3V)	**1 M NaOH**	**1 Sun**	**1.29 (1.6 V vs RHE)**	**Present work**
20% In_2Se_3/In_2O_3 (0V)	**1 M NaOH**	**1 Sun**	**0.99 (1.6 V vs RHE)**	**Present work**
20% In_2Se_3/In_2O_3 (-3V)	**1 M NaOH**	**1 Sun**	**1.91 (1.6 V vs RHE)**	**Present work**
In_2O_3/TiO_2	0.1 M Na_2SO_4	350W Xe lamp	0.65 (No mention)	[2]
In_2S_3/CdS/NiOOH	0.25 M Na_2S and 0.35 M Na_2SO_3	1 Sun	1.01 (1.23 V vs RHE)	[3]
In_2O_3/In_2S_3	1 M NaOH	300W Xe lamp	0.53 (1.23 V vs RHE)	[4]
N-doped In_2O_3	0.1 M Na_2SO_4	300W Xe lamp	0.2 (1.6 V vs RHE)	[5]
In_2O_3/Fe_2O_3	0.1 M NaOH	300W Xe lamp	0.04 (1.6 V vs RHE)	[6]
In_2O_3/ZnO	0.5 M Na_2SO_4	300W Xe lamp	0.36 (0.5 V vs Ag/AgCl)	[7]
In_2O_3/Carbon	Triethanolamine (8 vol%)	300W Xe lamp	0.04 (0.2 V vs Hg/Hg_2Cl_2)	[8]
In_2O_3/In_2S_3	0.5 M Na_2SO_4	1 Sun	0.14 (1.23 V vs RHE)	[9]
Ti-Fe_2O_3/In_2O_3	1 M NaOH	300W Xe lamp	1.33 (1.23 V vs RHE)	[10]

Ti-Fe_2O_3/In_2O_3	0.2 M K_2SO_4	1 Sun	0.52 (0.7 V vs RHE)	[11]
g-C_3N_4/In_2O_3	0.1 M Na_2SO_4	35W Xe lamp	1.3 (1.2 V vs RHE)	[12]
In_2O_3/CuO-0.03 wt% GNRs	1 M NaOH	1 Sun	1.51 (1.6 V vs RHE)	[1]

Supplementary references:

1. L. Shi, D. Benetti, Q. Wei and F. Rosei, *Small*, 2023, 2300606.
2. H. Yang, J. Tian, Y. Bo, Y. Zhou, X. Wang and H. Cui, *J. Colloid Interface Sci.*, 2017, **487**, 258-265.
3. L. Wei, J. Zhang and M. Ruan, *Appl. Surf. Sci.*, 2021, **541**, 148431.
4. H. Xu, H. Chen, S. Chen, K. Wang and X. Wang, *Int. J. Hydrogen Energy*, 2021, **46**, 32445-32454.
5. X. Gan, R. Zheng, T. Liu, J. Meng, R. Chen, X. Sun and X. Sun, *Chem. Eur. J.*, 2017, **23**, 7264-7271.
6. L. Wu, S. Ma, J. Li and X. Li, *Thin Solid Films*, 2021, **724**, 138600.
7. F.-Y. Su and W.-D. Zhang, *Mater. Lett.*, 2018, **211**, 65-68.
8. R. Li, L. Sun, W. Zhan, Y.-A. Li, X. Wang and X. Han, *J. Mater. Chem. A*, 2018, **6**, 15747-15754.
9. B. R. Lee, S. Choi, W. S. Cheon, J. W. Yang, M. G. Lee, S. H. Park and H. W. Jang, *Electron. Mater. Lett.*, 2022, **18**, 391-399.
10. S. Wang, Y. Wang, J. Li, S. Guo, C. Meng, L. Pan, J.-J. Zou, Y. Shi, L. Zhang and Z. Yin, *ACS Appl. Nano Mater.*, 2023, **6**, 20240-20250.
11. M. Szkoda, A. Ilnicka, Z. Zarach, D. Roda, A. Nowak and K. Trzciński, *J. Alloys Compd.*, 2023, **960**, 170924.
12. D. Sariket, A. Maity, S. Kundu and C. Bhattacharya, *J. Solid State Chem.*, 2022, **315**, 123484.